

CrystEngComm

Accepted Manuscript



This is an *Accepted Manuscript*, which has been through the Royal Society of Chemistry peer review process and has been accepted for publication.

Accepted Manuscripts are published online shortly after acceptance, before technical editing, formatting and proof reading. Using this free service, authors can make their results available to the community, in citable form, before we publish the edited article. We will replace this *Accepted Manuscript* with the edited and formatted *Advance Article* as soon as it is available.

You can find more information about *Accepted Manuscripts* in the [Information for Authors](#).

Please note that technical editing may introduce minor changes to the text and/or graphics, which may alter content. The journal's standard [Terms & Conditions](#) and the [Ethical guidelines](#) still apply. In no event shall the Royal Society of Chemistry be held responsible for any errors or omissions in this *Accepted Manuscript* or any consequences arising from the use of any information it contains.

PAPER

Self-triggered conformations of disulfide ensembles in coordination polymers with multiple metal clusters

3840 2546 Cite this DOI:
10.1039/x0xx00000x

Tien-Wen Tseng,^{*a} Tzuoo-Tsair Luo,^b Ying-Ru Shih,^{ab} Jing-Wen Shen,^{ab} Li-Wei Lee,^b Ming-Hsi Chiang,^{*b} and Kuang-Lieh Lu^{*b}

Received 00th December 2014,
Accepted 00th January 2015

DOI: 10.1039/x0xx00000x

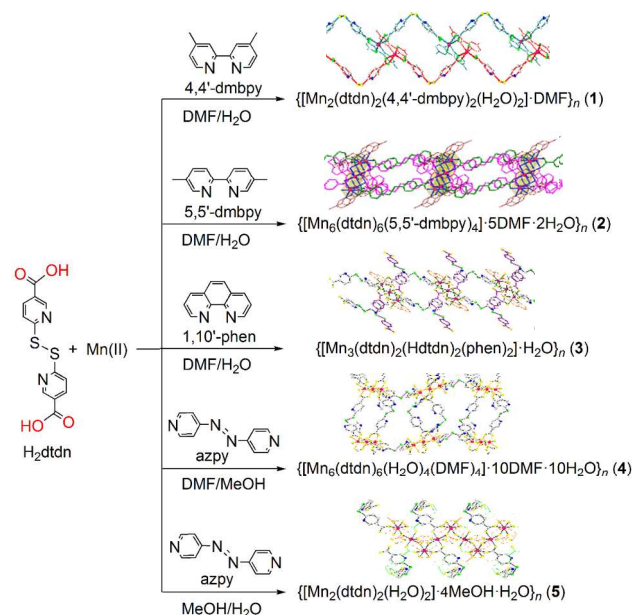
www.rsc.org/

Five coordination polymers, $\{[\text{Mn}_2(\text{dtdn})_2(4,4'\text{-dmbpy})_2(\text{H}_2\text{O})_2]\cdot\text{DMF}\}_n$ (**1**, $\text{dtdn} = 6,6'$ -thiodinicotinate), $\{[\text{Mn}_6(\text{dtdn})_6(5,5'\text{-dmbpy})_4]\cdot 5\text{DMF}\cdot 2\text{H}_2\text{O}\}_n$ (**2**), $\{[\text{Mn}_3(\text{dtdn})_2(\text{Hdtdn})_2(\text{phen})_2]\cdot\text{H}_2\text{O}\}_n$ (**3**), $\{[\text{Mn}_6(\text{dtdn})_6(\text{H}_2\text{O})_4(\text{DMF})_4]\cdot 10\text{DMF}\cdot 10\text{H}_2\text{O}\}_n$ (**4**), and $\{[\text{Mn}_2(\text{dtdn})_2(\text{H}_2\text{O})_2]\cdot 4\text{MeOH}\cdot \text{H}_2\text{O}\}_n$ (**5**) ($4,4'$ -dmbpy = $4,4'$ -dimethyl-2,2'-bipyridine, $5,5'$ -dmbpy = $5,5'$ -dimethyl-2,2'-bipyridine, phen = 1,10-phenanthroline), which were constructed under mild reaction conditions from a Mn(II) ion a twisted disulfide ligand H_2dtdn in the presence of different ancillary N-donor coligands and. These compounds show a variety of guest inclusion properties and interesting self-induced chirality. Compound **1** adopts 1D zigzag chains with mononuclear units that are mutually paired into a 1D ladder-like structure. Compound **2** consists of trinuclear clusters, and displays a 2D protuberant sheet with a (4,4)-sql topology. Compound **3** takes the form of a 1D double-stranded chain with rectangular loops comprised of trinuclear clusters, in which the Hdtdn^- ligands are dangling on both sides. Compound **4** adopts the form of a 2D network and exhibits a slightly undulating (4^4) topology that consists of trinuclear clusters, which are further hydrogen bonded into a 3D framework. Compound **5** features a 3D network consisting of 1D infinite metal oxide wires with the $[\text{Mn}_2(\text{dtdn})_2(\text{H}_2\text{O})_2]$ unit. The magnetic studies of compounds **2**, **3**, and **5** show that they have antiferromagnetic properties.

Introduction

The subjects of coordination polymers (CPs) have attracted considerable attention in recent years not only for the aesthetics of crystal architectures,¹ but also due to their potential applications, ranging from magnetism, luminescence to nonlinear optics, and gas storage.^{2–4} Crystal engineering directed towards the preparation of CPs containing multinuclear clusters with different shapes and topologies still confront great challenges, because their assembly might be triggered by more than one factors.⁵ Currently, considerable efforts have been expended toward taking advantage of the enhanced structural diversity imparted by carboxylate-containing ligands in combination with the N-donor species, which act as effective auxiliary ligands and/or exhibit a structure-directing effect, in

Scheme 1. Synthesis of compounds 1–5



^a Department of Chemical engineering, National Taipei University of Technology, Taipei 106, Taiwan. Fax: +886-2-2776-2383; Tel: +886-2-2771-2171 ext. 2538; E-mail: f10403@ntut.edu.tw

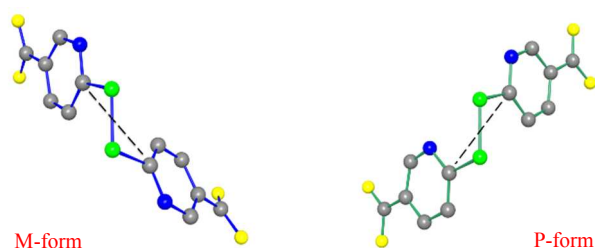
^b Institute of Chemistry, Academia Sinica, Taipei 115, Taiwan

† Electronic Supplementary Information (ESI) available: detailed experimental section and Figs. S1–S50. CCDC: 1037969–1037971 for **1–3**; 1037973(**4**); 1042806(**5**). For ESI and crystallographic

Table 1. Summary of crystal data and structure refinements for compounds 1–5

compound	1	2	3	4	5
empirical formula	C ₅₁ H ₄₇ Mn ₂ N ₉ O ₁₁ S ₄	C ₁₅₀ H ₁₆₂ Mn ₆ N ₃₀ O ₃₈ S ₁₂	C ₇₂ H ₄₄ Mn ₃ N ₁₂ O ₁₇ S ₈	C ₁₁₄ H ₁₆₂ Mn ₆ N ₂₆ O ₅₂ S ₁₂	C ₂₈ H ₃₄ Mn ₂ N ₄ O ₁₅ S ₄
formula weight	1200.10	3707.46	1770.49	3443.06	904.71
crystal system	Orthorhombic	Monoclinic	Triclinic	Triclinic	Monoclinic
space group	<i>Pbcn</i>	<i>P2₁</i>	<i>P-1</i>	<i>P-1</i>	<i>C2/c</i>
<i>a</i> (Å)	17.9446(5)	11.8071(2)	12.1946(7)	13.498(14)	22.739(5)
<i>b</i> (Å)	11.1704(3)	29.765(4)	12.5819(9)	15.220(16)	16.038(3)
<i>c</i> (Å)	27.2280(8)	13.1818(2)	14.6838(9)	20.51(2)	9.7046(19)
<i>α</i> (deg)	90	90	72.430(4)	90.775(13)	90
<i>β</i> (deg)	90	110.456(2)	69.157(4)	97.172(18)	94.00(3)
<i>γ</i> (deg)	90	90	62.887(4)	111.158(13)	90
<i>V</i> (Å ³)	5457.8(3)	4340.4(9)	1847.5(2)	3891(7)	3530.5(12)
<i>Z</i>	4	1	1	1	4
<i>T</i> (K)	200(2)	200(2)	200(2)	200(2)	153(2)
<i>λ</i> (Å)	0.71073	0.71073	0.71073	0.71073	0.71073
<i>D</i> _{calc} (g cm ⁻³)	1.461	1.418	1.591	1.469	1.702
<i>μ</i> (mm ⁻¹)	0.683	0.649	0.810	0.723	1.028
<i>F</i> ₀₀₀	2472	1918	899	1786	1856
GOF	1.057	1.064	1.026	0.912	1.030
<i>R</i> ₁ ^a (<i>I</i> > 2σ(<i>I</i>))	0.0272	0.0576	0.0563	0.0880	0.0401
w <i>R</i> ₂ ^b (<i>I</i> > 2σ(<i>I</i>))	0.0646	0.1490	0.1435	0.1794	0.0930
<i>R</i> ₁ ^a (all data)	0.0331	0.0848	0.1123	0.2078	0.0503
w <i>R</i> ₂ ^b (all data)	0.0682	0.1760	0.1966	0.1978	0.0990
Flack parameter		0.50(2)			

$${}^a R_1(F) = \frac{\sum \|F_o - |F_c|\|}{\sum |F_o|}, {}^b wR_2(F^2) = \frac{[\sum w(F_o^2 - F_c^2)^2 / \sum w(F_o^2)^2]}{1/2}$$

Chart 1. The enantiomers of the dtdn²⁻ ligand displaying chirality

efforts to construct new metal–organic compounds with polynuclear metal clusters.^{6–8} It is well known that disulfide-based compounds bearing a flexible –S–S– motif can display one of the most intriguing post-translational modifications and play a critical role in the folding structures of proteins.^{9–10} In general, the disulfide group is susceptible to *scission via in situ* cleavages of both S–S and S–C bonds,¹¹ and *in situ* exchange as a repository of reduced or oxidized disulfide bond moieties, which represents an important process in biological systems and *in situ* metal-mediated reactions.¹² In addition, disulfide-based ligands show axial chirality with the M- and P-forms of enantiomers (Chart 1), which provides an opportunity to produce some interesting metal complexes.¹³ Therefore, the preparation of metal–organic materials with variable disulfide ensembles for exploring their intrinsic biomimetic natures is currently an urgent and unexplored area of research.¹⁴

As part of our ongoing efforts in the design and synthesis of functional materials,¹⁵ herein we report on the preparation of some disulfide-based coordination polymers (Scheme 1), namely, $\{[\text{Mn}_2(\text{dtdn})_2(4,4'\text{-dmbpy})_2(\text{H}_2\text{O})_2]\cdot\text{DMF}\}_n$ (1), $\{[\text{Mn}_6(\text{dtdn})_6(5,5'\text{-dmbpy})_4]\cdot 5\text{DMF}\cdot 2\text{H}_2\text{O}\}_n$ (2),

$\{[\text{Mn}_3(\text{dtdn})_2(\text{Hdtdn})_2(\text{phen})_2]\cdot\text{H}_2\text{O}\}_n$ (3), $\{[\text{Mn}_6(\text{dtdn})_6(\text{H}_2\text{O})_4(\text{DMF})_4]\cdot 10\text{DMF}\cdot 10\text{H}_2\text{O}\}_n$ (4), and $\{[\text{Mn}_2(\text{dtdn})_2(\text{H}_2\text{O})_2]\cdot 4\text{MeOH}\cdot \text{H}_2\text{O}\}_n$ (5), which were synthesized via the reaction of a Mn(II) ion and a H₂dtdn ligand, a disulfide derivative of nicotinic acid, and different ancillary N-donor ligands (4,4'-dmbpy = 4,4'-dimethyl-2,2'-bipyridine, 5,5'-dmbpy = 5,5'-dimethyl-2,2'-bipyridine, phen = 1,10-phenanthroline, azpy = 4,4'-azopyridine). This work is noteworthy for several reasons: (i) the disulfide ensembles in Mn-based CPs can exist in versatile coordination modes that exhibit structurally biomimetic characteristics; (ii) a suitable impetus from the ancillary N-donor coligands directs the target coordination polymers comprised of mononuclear, trinuclear clusters and metal oxide wires, respectively; (iii) the sub-perturbations trigger an intrinsic axial chirality of the disulfide motifs in these intriguing CPs; (iv) the magnetic behaviors of 2, 3, and 5 were examined and correlated with their distinct multinuclear nodes. The focus of this work was on combining the freely twisted disulfide derivatives and different N-donor coligands to assembly the target CPs with diverse structures.¹⁶ To the best of our knowledge, such self-assembled CPs containing disulfide derivatives with the carboxylate moieties are currently rare.^{16–17}

Experimental section

General remarks. All reagents were purchased commercially and were used as received without further purification. Thermogravimetric analyses (TGA) were performed under nitrogen with a Perkin-Elmer Pyris 6 analyzer. The IR spectra were recorded in the 4000–400 cm⁻¹ region using KBr pellets on a Perkin-Elmer Paragon 1000 spectrometer. Elemental analyses were determined by a Perkin-Elmer 2400 elemental analyzer. The powder X-ray

Table 2. Selected bond lengths [Å] and angles [°] for 1–5

1							
S(1)–S(2)	2.0296(7)	Mn(1)–N(3)	2.245(2)	Mn(1)–N(4)	2.229(2)	O(4)#2–Mn(1)–O(5)	87.88(5)
Mn(1)–O(1)	2.320(2)	Mn(1)–O(5)	2.148(1)	O(5)–Mn(1)–O(1)	88.27(5)	O(2)–Mn(1)–N(4)	95.66(5)
Mn(1)–O(2)	2.253(1)	O(4)#2–Mn(1)–N(4)	90.78(5)	O(5)–Mn(1)–N(4)	118.87(5)	O(4)#2–Mn(1)–N(3)	159.86(5)
O(5)–Mn(1)–N(3)	89.13(5)	N(4)–Mn(1)–N(3)	73.31(5)	O(4)#2–Mn(1)–O(2)	96.11(5)	O(5)–Mn(1)–O(2)	145.25(5)
N(4)–Mn(1)–O(2)	95.66(5)	N(3)–Mn(1)–O(2)	97.66(5)	N(4)–Mn(1)–O(1)	148.87(5)	N(3)–Mn(1)–O(2)	97.66(5)
2							
S(1)–S(2)	2.019(3)	Mn(2)–O(9)	2.192(4)	Mn(3)–O(6A)	2.062(6)	O(7A)#3–Mn(2)–O(11)#1	88.7(6)
Mn(1)–O(1)	2.243(5)	Mn(2)–O(4)#1	2.175(4)	Mn(3)–O(12)#1	2.095(5)	O(11)#1–Mn(2)–O(2)	86.5(2)
Mn(1)–O(2)	2.307(4)	Mn(2)–O(5A)	2.20(1)	Mn(3)–O(10)	2.250(5)	O(6A)–Mn(3)–O(10)	155.5(6)
Mn(1)–N(7)	2.258(6)	Mn(2)–O(7A)#3	2.17(2)	Mn(3)–N(9)	2.216(6)	O(4)#3–Mn(2)–O(9)	87.2(2)
Mn(1)#1–O(3)	2.100(5)	Mn(2)–O(11)#1	2.175(4)	Mn(3)–N(10)	2.248(6)	O(6A)–Mn(3)–N(9)	101.8(3)
Mn(1)–N(8)	2.200(6)	N(8)–Mn(1)–N(7)	72.9(2)	N(8)–Mn(1)–O(2)	147.8(2)	N(9)–Mn(3)–N(10)	73.7(2)
3							
S(1)–S(2)	2.032(2)	Mn(2)–O(6)	2.133(4)	N(6)–Mn(1)–N(5)	74.4(2)	O(3)#3–Mn(1)–N(5)	172.6(2)
Mn(1)–N(5)	2.256(4)	Mn(2)–O(2)	2.184(4)	O(5)–Mn(1)–N(5)	87.7(2)	O(5)–Mn(1)–N(6)	97.0(2)
Mn(1)–O(2)	2.215(4)	Mn(2)–O(4)#1	2.168(4)	N(5)–Mn(1)–O(1)	89.1(2)	O(6)–Mn(2)–O(4)#3	87.1(2)
Mn(1)–N(6)	2.228(5)	O(5)–Mn(1)–O(2)	117.4(2)	O(2)–Mn(1)–N(6)	172.6(2)	O(6)–Mn(2)–O(2)#2	97.3(2)
Mn(1)–O(1)	2.447(4)	O(2)–Mn(1)–N(6)	140.0(2)	O(3)#1–Mn(1)–N(5)	95.5(2)	O(6)#2–Mn(2)–O(2)#2	82.7(2)
Mn(1)–O(3)#1	2.081(4)	N(6)–Mn(1)–O(1)	88.2(2)	O(2)–Mn(1)–O(1)	56.2(1)	O(4)#1–Mn(2)–O(2)#2	89.4(2)
4							
S(1)–S(2)	2.035(4)	Mn(2)–O(6)	2.219(8)	Mn(4)–O(10)	2.131(7)	O(1)–Mn(2)–O(6)	84.7(3)
S(3)–S(4)	2.064(5)	Mn(2)–O(1)	2.137(7)	Mn(4)–O(11)#1	2.141(7)	O(9)–Mn(3)–O(12)#1	96.0(3)
S(5)–S(6)	2.040(4)	Mn(3)–O(3)	2.283(6)	O(6)–Mn(1)–O(16)	86.9(4)	O(9)–Mn(3)–O(14)	86.4(3)
Mn(1)–O(2)	2.147(7)	Mn(3)–O(9)	2.107(6)	O(2)–Mn(1)–O(5)	162.4(3)	O(9)–Mn(3)–O(15)	106.2(3)
Mn(1)–O(5)	2.385(8)	Mn(3)–O(4)	2.325(7)	O(7)#1–Mn(1)–O(5)	88.1(3)	O(15)–Mn(3)–O(14)	89.7(4)
Mn(1)–O(13)	2.160(6)	Mn(3)–O(15)	2.168(8)	O(2)–Mn(1)–O(6)	106.1(3)	O(10)–Mn(4)–O(3)	87.9(3)
Mn(1)–O(7)#1	2.136(7)	Mn(4)–O(3)	2.235(7)	O(13)–Mn(1)–O(6)	150.0(3)	O(11)#1–Mn(4)–O(3)	92.9(2)
5							
S(3)–S(4)	2.023(1)	Mn(2)–O(5)	2.202(2)	O(1)#1–Mn(1)–O(3)#4	93.61(7)	O(2)#6–Mn(2)–O(2)	159.8(1)
Mn(1)–O(1)	2.107(2)	Mn(2)–O(3)#3	2.193(2)	O(1)–Mn(1)–O(4)#2	91.47(7)	O(2)#6–Mn(2)–O(3)#5	93.83(8)
Mn(1)–O(4)#2	2.199(2)	Mn(2)–O(2)	2.125(2)	O(2)–Mn(2)–O(3)#2	93.83(9)	O(2)–Mn(2)–O(5)#6	79.08(9)
Mn(1)–O(3)#4	2.245(2)	O(1)#1–Mn(1)–O(4)#2	88.53(7)	O(2)–Mn(2)–O(5)	87.8(1)	O(3)#2–Mn(2)–O(5)#6	88.86(9)

^aSymmetry transformations used to generate equivalent atoms, for **1**: #2 $x, -y + 1, z - 1/2$; for **2**: #1 $x - 1, y, z - 1$; #3 $-x + 1, y + 1/2, -z + 1$; for **3**: #1 $x + 1, y - 1$; #2 $-x + 2, -y, -z$; #3 $-x + 1, -y + 1, -z$; for **4**: #1 $x - 1, y, z$; for **5**: #2 $-x + 3/2, -y + 1/2, -z + 2$; #3 $x + 1/2, y - 1/2, z$; #4 $-x + 3/2, y - 1/2, -z + 3/2$; #5 $x + 1/2, -y + 1/2, z + 1/2$; #6 $-x + 2, y, -z + 5/2$.

diffraction (PXRD) patterns obtained on a MPD Philips Analytical diffractometer at 40 kV, 30 mA for Cu $K\alpha$ ($\lambda = 1.5406$ Å). Solid-state photoluminescence was recorded on a Hitachi F4500 spectrometer. Temperature-dependant magnetic measurements were carried out on a MPMS XL-7 SQUID magnetometer. Magnetic susceptibility data were collected in the temperature range of 2–300 K. Magnetization data under various strength of magnetic field were collected at 1.8 K. Diamagnetic correction was made with Pascal's constants.

Synthesis of $\{[\text{Mn}_2(\text{dtdn})_2(4,4'\text{-dmbpy})_2(\text{H}_2\text{O})_2]\cdot\text{DMF}\}_n$ (**1**)

A mixture of 6,6'-dithiodinicotinic acid (H_2dtdn) (15.5 mg, 0.0499 mmol), 4,4'-dimethyl-2,2'-bipyridine (4,4'-dmbpy, 9.21 mg, 0.0500 mmol) and manganese(II) nitrate hexahydrate (29.0 mg, 0.101 mmol) was dissolved in a DMF solution ($\text{H}_2\text{O}:\text{DMF} = 2.0 \text{ mL}:\text{5.0 mL}$). The resulting solution was kept at 50 °C for two weeks. The light-yellow hexagonal crystals of **1** were separated by filtration, washed with water and DMF, and dried in air. Yield: 84.2% (25.2 mg, 0.0210 mmol) based on H_2dtdn . Elemental anal. Calcd for $\text{C}_{51}\text{H}_{47}\text{N}_9\text{O}_{11}\text{S}_4\text{Mn}_2$:

C, 51.04; H, 3.92; N, 10.50. Found: C, 51.16; H, 4.12; N, 10.57. IR (KBr, cm^{-1}): 3258(w), 3050(w), 2927(w), 1686(s), 1617(w), 580(s), 1542(w), 1529(w), 1486(w), 1448(w), 1408(w), 1387(s), 1358(m), 1302(w), 1288(w), 1269(w), 1243(w), 1156(m), 1128(w), 1096(s), 1034(w), 1016(m), 860(s), 832(s), 785(s), 550(m), 529(m), 514(m).

Synthesis of $\{[\text{Mn}_6(\text{dtdn})_6(5,5'\text{-dmbpy})_4]\cdot 5\text{DMF}\cdot 2\text{H}_2\text{O}\}_n$ (**2**)

A mixture of H_2dtdn (15.5 mg, 0.0499 mmol), 5,5'-dimethyl-2,2'-bipyridine (5,5'-dmbpy, 9.20 mg, 0.0500 mmol) and manganese(II) nitrate hexahydrate (29.1 mg, 0.101 mmol) was mixed with a DMF solution ($\text{H}_2\text{O}:\text{DMF} = 0.5 \text{ mL}:\text{5.0 mL}$). The resulting solution was kept at 50 °C for 17 days. The pale yellow rectangular crystals of **2** were collected by filtration, washed with water and DMF, and dried in air. Yield: 58.2% (15.8 mg, 0.00484 mmol) based on H_2dtdn . Elemental anal. Calcd for $\text{C}_{150}\text{H}_{1162}\text{N}_{30}\text{O}_{38}\text{S}_{12}\text{Mn}_6$: C, 48.59; H, 4.40; N, 11.33. Found: C, 48.10; H, 4.14; N, 10.70. IR (KBr, cm^{-1}): 3407(m), 3046(w), 2925(w), 1669(s), 1609(s), 1579(s), 1547(m), 1502(w),

1479(m), 1398(s), 1357(s), 1269(m), 782(s), 733(m), 522(m).

Synthesis of $\{[\text{Mn}_3(\text{dtdn})_2(\text{Hdtdn})_2(\text{phen})_2]\cdot\text{H}_2\text{O}\}_n$ (3)

A mixture of H_2dtdn (15.4 mg, 0.0494 mmol), 1,10-phenanthroline hydrate (10.0 mg, 0.0505 mmol) and manganese(II) nitrate hexahydrate (29.6 mg, 0.103 mmol) was mixed with a DMF solution ($\text{H}_2\text{O}:\text{DMF} = 2.0 \text{ mL}:5.0 \text{ mL}$). The resulting solution was kept at 50 °C for 14 days. The pale yellow hexagonal crystals of **3** were collected by filtration, washed with water and DMF, and dried in air. Yield: 65.9% (14.4 mg, 0.00814 mmol) based on H_2dtdn . Elemental anal. Calcd for $\text{C}_{72}\text{H}_{44}\text{N}_{12}\text{O}_{17}\text{S}_8\text{Mn}_3$: C, 48.84; H, 2.50; N, 9.50. Found: C, 48.65; H, 2.49; N, 9.49. IR (KBr, cm^{-1}): 3392(s), 3069(w), 1599(s), 1517(m), 1424(m), 1387(s), 1096(m), 847(s), 729(s), 723(s).

Synthesis of $\{[\text{Mn}_6(\text{dtdn})_6(\text{H}_2\text{O})_4(\text{DMF})_4]\cdot 10\text{DMF}\cdot 10\text{H}_2\text{O}\}_n$ (4)

A mixture of H_2dtdn (15.5 mg, 0.0499 mmol), 4,4'-azopyridine (9.2 mg, 0.050 mmol), and manganese(II) nitrate hexahydrate (29.5 mg, 0.103 mmol) was dissolved in a DMF solution ($\text{H}_2\text{O}:\text{MeOH}:\text{DMF} = 2.0 \text{ mL}:1.0 \text{ mL}:5.0 \text{ mL}$). The resulting solution was kept at 50 °C for 14 days. The orange block crystals of **4** were collected by filtration, washed with methanol and DMF, and dried in air. Yield: 82.1% (17.8 mg, 0.00683 mmol) based on H_2dtdn . Elemental anal. Calcd for $\text{C}_{114}\text{H}_{162}\text{Mn}_6\text{N}_{26}\text{O}_{52}\text{S}_{12}$: C, 39.77; H, 4.74; N, 10.58. Found: C, 40.00; H, 4.20; N, 10.50. IR (KBr, cm^{-1}): 3365(w), 3047(w), 2503(w), 1660(s), 1652(w), 1605(w), 1581(s), 1538(m), 1403(s), 1355(m), 1161(m), 1097(s), 863(s), 845(m), 781(s), 664(s), 519(m).

Synthesis of $\{[\text{Mn}_2(\text{dtdn})_2(\text{H}_2\text{O})_2]\cdot 4\text{MeOH}\cdot \text{H}_2\text{O}\}_n$ (5)

A mixture of H_2dtdn (15.5 mg, 0.0499 mmol), 4,4'-azopyridine (9.3

mg, 0.051 mmol), KOH (5.7 mg, 0.10 mol), and manganese(II) nitrate hexahydrate (28.8 mg, 0.100 mmol) was dissolved in a methanol solution ($\text{MeOH}:\text{H}_2\text{O} = 5.0 \text{ mL}:1.0 \text{ mL}$). The resulting solution was kept at 50 °C for a week. The orange needle crystals of **5** were separated by filtration, washed with water and MeOH, and dried in air. Yield: 80.6 % (18.3 mg, 0.0201 mmol) based on H_2dtdn . Elemental anal. Calcd for $\text{C}_{28}\text{H}_{34}\text{Mn}_2\text{N}_4\text{O}_{15}\text{S}_4$: C, 37.17; H, 3.79; N, 6.19. Found: C, 36.09; H, 3.05; N, 7.47. IR (KBr, cm^{-1}): 3354(w), 3088(w), 1604(s), 1586(s), 1549(s), 1450(m), 1410(s), 1378(s), 1356(s), 1274(m), 1159(s), 1098(s), 1025(m), 844(m), 783(s), 568(m), 524(m).

Crystal structure determination

Single-crystal X-ray diffraction data were collected using a Nonius Kappa CCD diffractometer, equipped with Mo $K\alpha$ radiation ($\lambda = 0.71073 \text{ \AA}$). The structures were solved using direct methods. The hydrogen atoms of the ligands were placed in calculated positions with isotropic thermal parameters and were included in the structure factor calculations in the final stage of full-matrix least-squares refinement. All calculations were performed using the SHELX-97 program packages.¹⁸ The hydrogen atoms attached to carbon atoms were assigned by geometrical calculation and refined as a riding model. The hydrogen atoms attached to oxygen atoms were located from the difference Fourier maps. Because the crystal structure of compound **4** contains many disordered guest molecules that cannot be modelled and refined well, the "SQUEEZE" tool was used to take the scattering of a disordered solvent into account.¹⁹ Crystal data and structure refinement data for compounds **1–5** are summarized in Table 1, and the selected bond lengths and angles are listed in Table 2.

Results and discussion

Chart 2. Coordination modes of the dtdn^{2-} ligand

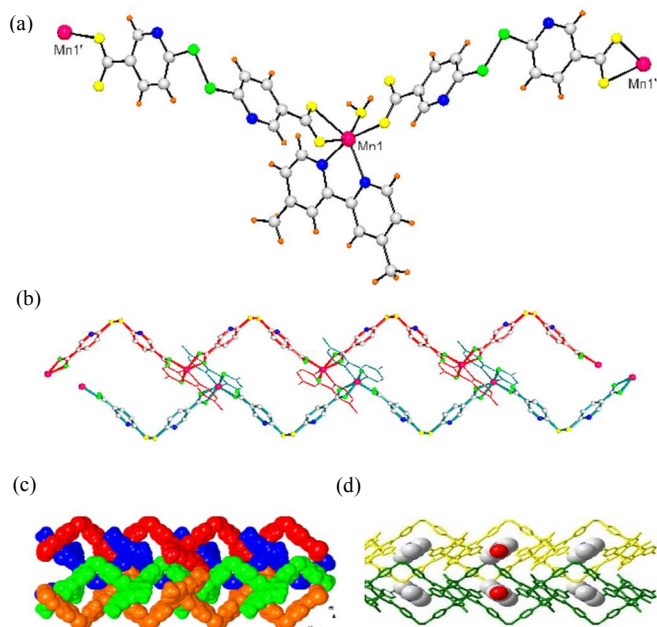
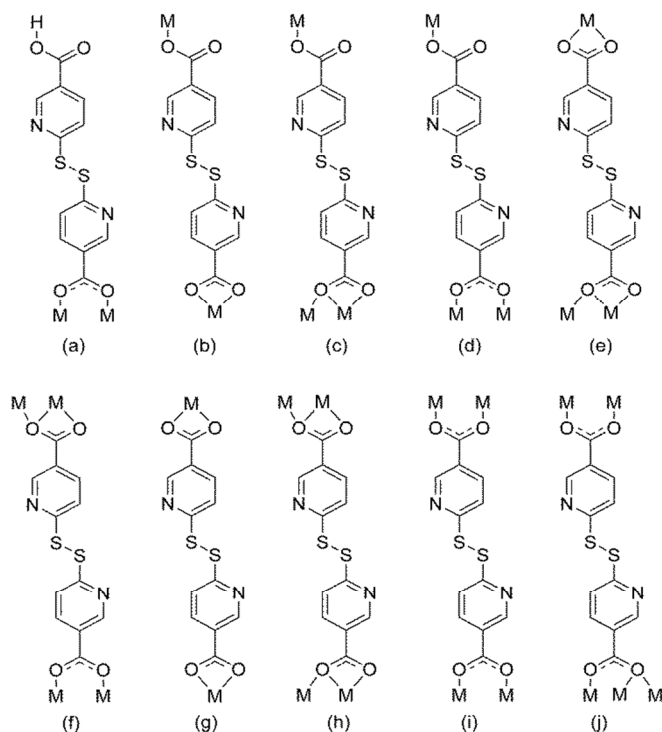


Figure 1. Structures of **1**: (a) coordination environments of Mn(II) centers; (b) a pair of zigzag chains packed into a 1D ladder-like structure viewed along the *b* axis; (c) the ladders are stacked into a 2D network in space-filling mode; (d) DMF molecules are filled in the cavities.

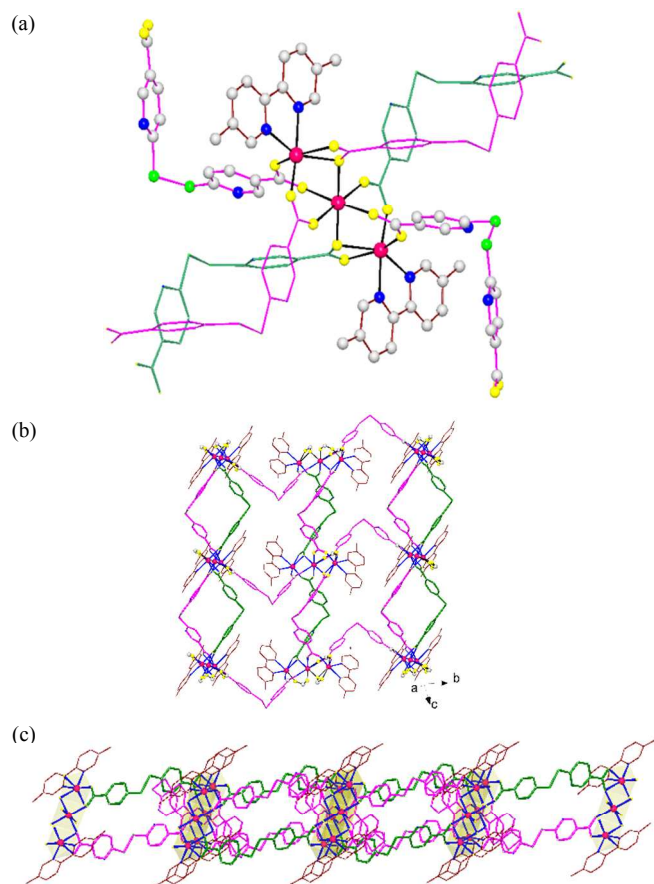


Fig. 2 (a) Coordination environments of Mn(II) ions in **2**. (b) A 2D protuberant chiral sheet with a (4,4)-**sql** topology containing the trinuclear clusters. (c) Side view of a sheet along the *c* axis.

Structure of $\{[\text{Mn}_2(\text{dtdn})_2(4,4\text{'-dmbpy})_2(\text{H}_2\text{O})_2]\cdot\text{DMF}\}_n$ (**1**)

A single-crystal X-ray diffraction analysis revealed that compound **1** crystallizes in the orthorhombic space group *Pbcn* and has a 1D chain structure. The Mn(II) ion is coordinated to one chelated 4,4'-dmbpy, two carboxylates of two distinct dtdn²⁻ ligands, and one coordinated water molecules in a distorted octahedral fashion (Fig. 1a). Two Mn(II) centers are bridged by a dtdn²⁻ ligand employing a η²-carboxylate (O2, O1) and a η¹-carboxylate (O4) group (Fig. S1 in ESI[†]). It is interesting that, owing to the intrinsic pseudo chirality of the dtdn²⁻ ligand, the dtdn²⁻ ligand can exhibit in P- or M-conformations, resulting in the formation of a zig-zag polymeric chain (Fig. S2 in ESI[†]). Furthermore, a couple of zigzag chains, bearing P- and M-conformations are paired together via hydrogen bonding interactions, leading to the formation of a 1D ladder-like structure (Fig. 1b and Fig. S3 in ESI[†]). The bond distances of Mn–O fall in the range of 2.32–2.12 Å. One chelated 4,4'-dmbpy (N3, N4) is coordinated to the Mn(II) center (the average Mn–N bond distances are 2.24 Å). The dtdn²⁻ ligand displays Type b coordination mode (Chart 2 and Fig. S4 in ESI[†]). A ladder-like structure is formed that is connected via and π–π stacking interactions from the pyridyl rings, which is further stacked into a 2D sheet (Fig. 1c and Fig. S5 in ESI[†]). This 2D network presents unique rectangular spaces with a window size of 7.52 × 12.29 Å², where one guest DMF

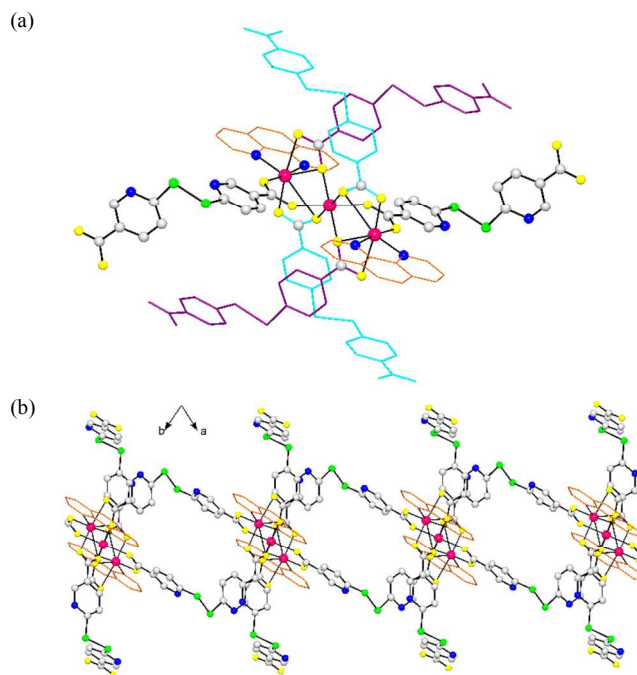


Fig. 3 (a) Coordination environments of Mn(II) centers in **3**. (b) A 1D double-stranded rod comprising of the rectangular loops and dangling with the Hddtn ligands on both sides of chain.

molecule is included and disordered about a twofold axis.

Structure of $\{[\text{Mn}_6(\text{dtdn})_6(5,5\text{'-dmbpy})_4]\cdot 5\text{DMF}\cdot 2\text{H}_2\text{O}\}_n$ (**2**)

The asymmetric unit of compound **2** contains three Mn(II) ions, three dtdn²⁻ ligands, two 5,5'-dmbpy ligands, and one guest DMF molecule (Fig. 2a and Fig. S6 in ESI[†]). As shown in Fig. S6, the Mn1 atom is coordinated with three dtdn²⁻ ligands (O3, O8, O1, O2) and two N atoms from 5,5'-dmbpy ligand in a MnO₄N₂ form. The Mn2 atom surrounded by six different carboxylate groups and that of Mn3 atom is almost the same as the Mn1 atom. Three Mn(II) atoms are bridged together by six dtdn²⁻ ligands to form a trinuclear cluster unit that is formed via two μ₂,η²-carboxylates (O2) and four μ₂,η¹-carboxylates (O3, O4, O7, O8). The separation distances between Mn···Mn are 3.55 and 3.57 Å, respectively (Fig. S7 in ESI[†]). It is noteworthy that four dtdn²⁻ ligands with flexible characteristics exhibit P- and M-forms, as a result, they are paired to link the adjacent clusters. However, the other two dtdn²⁻ ligands exist only in the M-form, leading to the formation of a 2D protuberant chiral sheet (Fig. 2b). The coordination modes of the dtdn²⁻ ligand display Types f and i (Chart 2 and Fig. S9 in ESI[†]). Finally, these adjacent 2D layers are regularly packed into a 3D framework (Fig. S10 in ESI[†]) via π–π stacking interactions (two pyridyl groups of two dtdn²⁻ ligands separated with 3.58 and 3.65 Å). Furthermore, the trinuclear unit can be regarded as a 4-connected node, thus it is further propagated into a 2D protuberant chiral sheet with a (4,4)-**sql** topology (Fig. S11 in ESI[†]). In the 3D structure, there are 1D open channels with a window size of 14.30 × 14.92 Å², that is filled with guest DMF molecules.

Structure of $\{[\text{Mn}_3(\text{dtdn})_2(\text{Hddtn})_2(\text{phen})_2]\cdot\text{H}_2\text{O}\}_n$ (**3**)

Compound **3** crystallizes in the triclinic space group *P*-1 and is

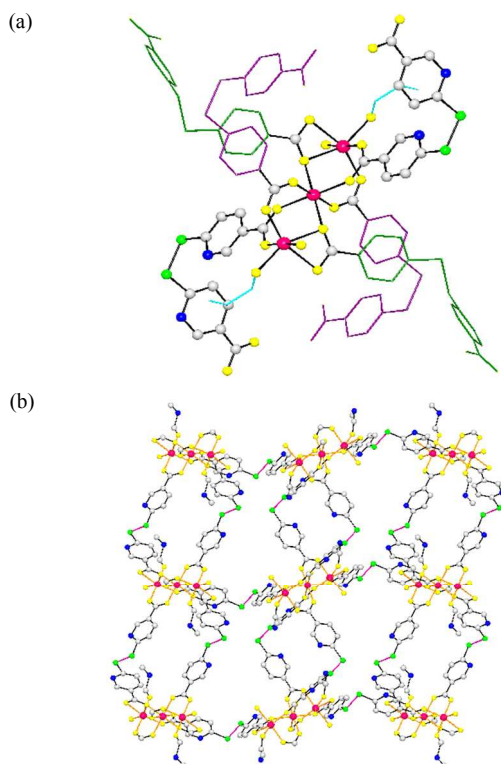


Fig. 4 Structures of **4**: (a) local coordination environments of the Mn(II) ions, (b) a view of a 2D undulated network.

comprised of a trinuclear cluster $[\text{Mn}_3(\text{dtdn})_2(\text{Hdtdn})_2(\text{phen})_2]$ unit. There are two crystallographically independent Mn atoms (Fig. 3a and Fig. S12 in ESI[†]). The Mn1 atom is located at both sides of the trinuclear cluster and coordinated by one η^2 -carboxylate (O1, O2), two μ_2, η^2 -carboxylate groups (O3, O5), and one phen ligand (N5, N6) in a distorted octahedral geometry. The central Mn2 atom is on an inversion center and coordinated in a MnO_6 manner by six dtdn^{2-} ligands (O2, O4, and O6). Three Mn(II) atoms are bridged by four μ_2, η^1 -carboxylate groups and two μ_2, η^2 -carboxylate groups, and the separation distance of $\text{Mn1} \cdots \text{Mn2}$ is 3.42(1) Å (Fig. S13 in ESI[†]). When four bridging dtdn^{2-} ligands are employed to link two adjacent trinuclear clusters, a 1D double-stranded rod comprised of the rectangular loops is formed. In addition, there are two terminal carboxylate motifs from two Hdtdn^- ligands on the trinuclear cluster that did not participate in the coordination (highlighted in pale blue in Fig. 3a), thus, they are dangling on both sides of a 1D rod-like structure (Fig. 3b). The dtdn^{2-} ligands display a P-conformation and their coordination modes are Type f, whereas the Hdtdn^- ligand displays a P-conformation and Type a (Fig. S15 in ESI[†]). In addition, these rods are stacked in an AAA manner (Fig. S16 in ESI[†]), leading to the formation of a 2D sheet via the π - π interactions (between pyridyl rings is 3.73(1) Å and that for the phen rings is 3.75(1) Å (Fig. S16 and S17 in ESI[†]). The window size of each loop is 14.68(1) \times 12.58(1) Å², in which one guest water molecule is included (Fig. S18 in ESI[†]). It is noteworthy that the phen coligand was located on both sides of the trinuclear cluster. When the extension of the network is blocked, only a 1D double-strained rod is formed.

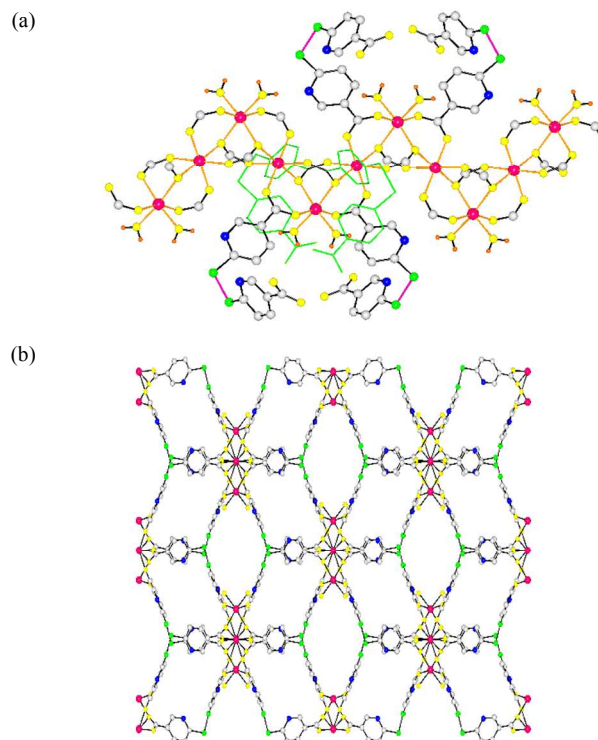


Fig. 5 Structures of **5**: (a) a 1D infinite Mn(II)-oxide wire formed by connecting through the bridging dtdn^{2-} ligands, (b) perspective view along the *c* axis.

Structure of $\{[\text{Mn}_6(\text{dtdn})_6(\text{H}_2\text{O})_4(\text{DMF})_4] \cdot 10\text{DMF} \cdot 10\text{H}_2\text{O}\}_n$ (**4**)

Compound **4** crystallizes in the triclinic space group $P\bar{1}$ and has a 2D framework (Fig. 4). The asymmetric unit contains two similar trinuclear clusters with the $[\text{Mn}_3(\text{dtdn})_3(\text{H}_2\text{O})_2(\text{DMF})_2]$ units (Mn1–Mn2–Mn1, Mn3–Mn4–Mn3) and three DMF molecules. The Mn2 and Mn4 atoms lie on inversion centres and the $\text{Mn1} \cdots \text{Mn2}$ and $\text{Mn3} \cdots \text{Mn4}$ separation distances of are 3.65(1) and 3.60(1) Å, respectively (Fig. S20 in ESI[†]). In addition, the coordinated DMF and water molecules (O13, O14, O23, O16) are located on both sides of the trinuclear clusters (Mn1 and Mn3). The intrinsic steric hindrance from the coordinated DMF molecules that are located on both terminal coordination sides of each clusters, affects the conformations of the dtdn^{2-} ligands, thus, resulting in the formation of a 1D horizontal zig-zag chain with an M-form (Fig. S21 in ESI[†]). Two neighbour chains are linked *via* the vertical dtdn^{2-} ligands to adopt P- and M-forms that are paired together, leading to the formation of an undulating, 2D network (Fig. 4b). The dtdn^{2-} ligands display coordination Types i and f, and the torsion angles of the former one are 104.6° and 104.9°, whereas, that of the later one are 103.2° and 105.8° (Fig. S22 in ESI[†]). π - π Stacking interactions from the adjacent pyridyl units of the dtdn^{2-} ligands are present between these layers with a distance of 3.33(1) Å (Fig. S23 in ESI[†]). In addition, the coordinated water molecules (O14, O16) are also hydrogen bonded to the acceptor atoms (O17, N2) of DMF and the dtdn^{2-} ligand, respectively, the 2D layers are further regularly packed to produce 3D network (Fig. 4c). There are ten DMF and ten H_2O

guest molecules that present in the cavities of the 3D network (Fig. S24 in ESI[†]).

Structure of $\{[\text{Mn}_2(\text{dtdn})_2(\text{H}_2\text{O})_2] \cdot 4\text{MeOH} \cdot \text{H}_2\text{O}\}_n$ (**5**)

Compound **5** crystallizes in the monoclinic space group $C2/c$ and has a 3D framework structure. The asymmetric unit consists of two Mn^{II} centers, two bridging dtdn^{2-} ligands, two coordinated water molecules, and four disordered guest methanol and two water molecules (Fig. 5a and Fig. S25 in ESI[†]). The Mn1 atom is on an inversion centre and bound to six carboxylate oxygen atoms from distinct bridging dtdn^{2-} ligands. The Mn2 atom lies on a twofold axis and is bound to four carboxylate oxygen atoms (O_2 , O_3) from four dtdn^{2-} ligands and two coordinated water molecules (O_5). The two nonequivalent Mn atoms adopt a distorted MnO_6 octahedral geometry. The Mn atoms are bridged by three carboxylate motifs of dtdn^{2-} ligands in μ_2, η^1 - and μ_2, η^2 -manners, leading to the formation of a 1D polymeric Mn(II)-oxide chain, in which the separation distance of $\text{Mn1} \cdots \text{Mn2}$ is 3.64(1) Å (Fig. S26 in ESI[†]). All of the Mn–O distances are in the range between 2.11 and 2.25 Å. It should be noted that each dtdn^{2-} ligand is bridged to five Mn(II) centers displaying Type j connecting mode (Fig. S28 in ESI[†]). The guest methanol and water molecules are encapsulated within the voids (Fig. S30 in ESI[†]). In addition, compound **5** shows large void volume with 28.9% ($1123.6 \text{ \AA}^3 / 3891.0 \text{ \AA}^3$).

Effective strategy for the syntheses of 1–5

As shown in Scheme 1, compounds **1–5** were synthesized by reacting with $\text{Mn}(\text{NO}_3)_2 \cdot 6\text{H}_2\text{O}$ and the H_2dtdn ligand at 50 °C. In a comparison of five complexes, the flexible dtdn^{2-} ligand provides multiple coordination modes, which facilitates the formation of the prospective secondary building units (SBUs). Thus, these SBUs sequentially could be comprised in the target structures containing the multiple-connected networks with chiral structures via the bridged dtdn^{2-} ligands.¹⁶ In addition, the introduction of organic ligands containing N-donors, possessing subtle chelating effect and/or steric hindrance, offers a tremendous impetus to influence the nuclearity and the coordination of the metal centers and to stabilize the solid-state structures of **1–3**. Furthermore, compounds **4** and **5** were prepared in the presence of an azpy species, a pyridyl derivative that could function as an organic base and/or template. It should be noted that compounds **4** and **5** are synthesized in similar conditions except that different solvent systems (DMF/MeOH and MeOH/ H_2O) were used, where the solvents play a vital role in the assembly of coordination polymers. In particular, we examined several alternated routes in the absence of azpy, but none were successful in the construction of structures **4** and **5**. The approach based on a combination of the disulfide derivative, H_2dtdn and related rigid N-donor ligands has enriched the assembly of CPs with diverse structures possessing the mononuclear, trinuclear clusters, and infinite metal oxide wires, respectively. To the best of our knowledge, the use of the disulfide-based ligand, H_2dtdn , and accompanying related coligands with different steric hindrance, which react under mild conditions, to tune the target structures has never been documented to date.¹⁶

It is noteworthy that the 1D ladder-like structure of **1** consists

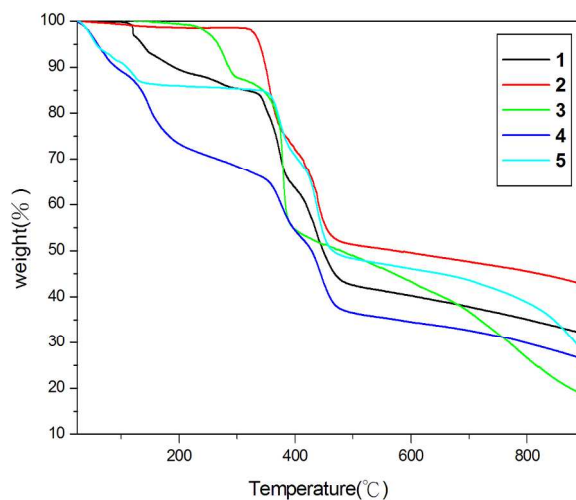


Fig. 6 The TGA profiles of compounds 1–5.

of several zigzag chains, and the dtdn^{2-} ligands adopt P- and M-conformations. Whereas, among the six dtdn^{2-} ligands of a trinuclear cluster of **2**, four dtdn^{2-} ligands exhibit P- and M-forms that are paired to link the adjacent clusters, the other two dtdn^{2-} ligands exist only in the M-form, resulting in the formation of a 2D chiral sheet. Compound **3** takes the form of a 1D double-stranded rod with dangling Hdtdn^- ligands and employs four bridging dtdn^{2-} ligands with a P-form to link adjacent trinuclear clusters and the Hdtdn^- ligands exhibit a P-form. The 2D undulated network of **4** consists of a 1D horizontal zig-zag chain in an M-form and the vertical dtdn^{2-} ligands adopt P- and M-forms that are paired together. Thus, these SBUs sequentially could make up the target structures containing the multiple-connected networks with chiral structures via the bridging dtdn^{2-} ligands.¹⁵ Furthermore, the diversity of structures of compounds **1–5** are good examples of the intrinsic twisted characteristics of such disulfide ensembles, which resembles the unique folded structures in cysteine peptides and protein substrates.

Thermogravimetric analyses and PXRD measurements

The results of thermogravimetric analyses (TGA) of **1–5** are shown in Fig. 6. For compound **1**, a weight loss of 13.2 % (calculated at 14.3 %) in the range of 80–200 °C was found, which can be attributed to the loss of one coordinated water and one guest DMF molecules. The TGA profiles of complexes **2** and **3** indicate that the guest DMF and water molecules are removed at temperatures below 150 °C, no further significant weight loss occurs until the temperatures reach 332 and 313.5 °C, respectively, indicating their highly thermal stability. The results of **4** indicate that the coordinated and guest water, and DMF molecules are easily lost and the complex gradually decomposes upon increasing temperature. Whereas for **5**, a weight loss of 14.2 % (calculated at 14.3 %) in the range of 40–150 °C is due to the loss of the water and methanol molecules, after which, it is thermally stable to a temperature of up to 350 °C, which can mainly be attributed to its 3D rigid network. Powder X-ray diffraction (PXRD) patterns were used to check the purity of compounds **1–5** (Figs. S36–S40 in ESI[†]). The results show that all of the peaks in the as-synthesized patterns at the room temperature are completely consistent with simulated patterns.

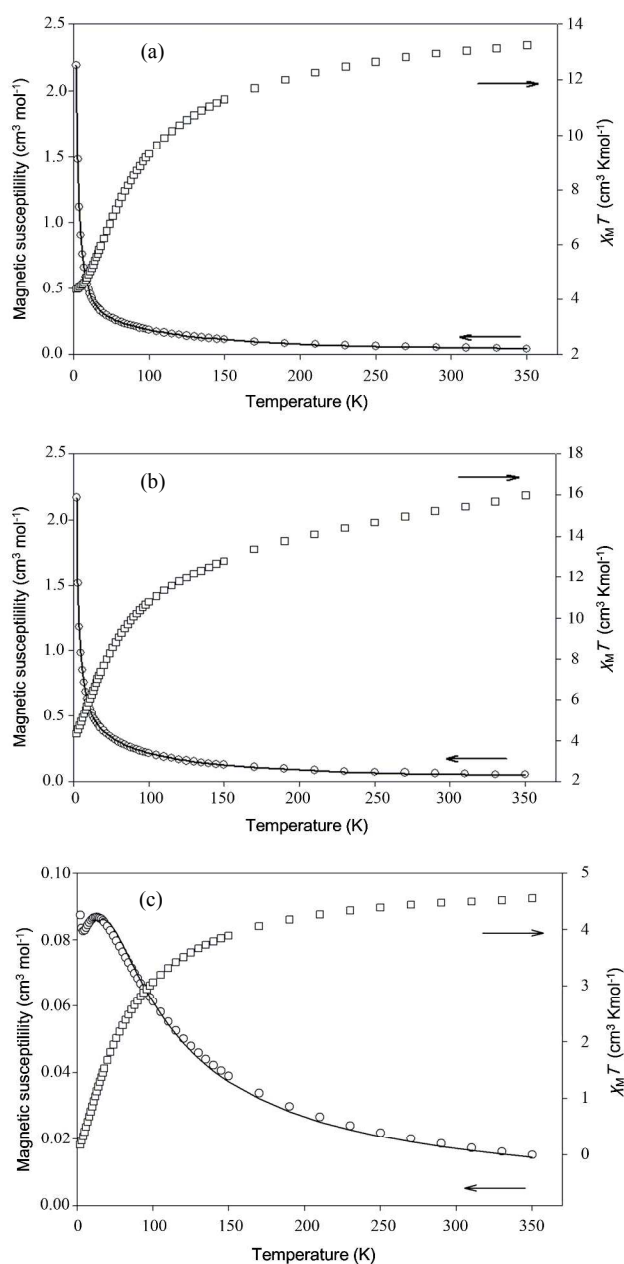


Fig. 7 Plots of χ_M vs. T (\circ) and $\chi_M T$ vs. T (\square) for the powder sample of compounds: **2** (a); **3** (b); **5** (c).

Magnetic studies of compounds **2**, **3**, and **5**

Magnetic susceptibility data for powder samples **2**, **3**, and **5** were collected in the temperature range of 2–300 K, respectively (Fig. 7). For compounds **2** and **3**, their corresponding $\chi_M T$ values are 13.244 and 15.984 $\text{cm}^3 \text{K mol}^{-1}$ at 300 K, respectively. These values are higher than that of the spin-only value of 13.125 $\text{cm}^3 \text{K mol}^{-1}$. The magnetic susceptibility data of **2** were fitted to give the Curie constant $C = 14.41 \text{ cm}^3 \text{K mol}^{-1}$ and the Weiss constant $\theta = -27.6 \text{ K}$ (Fig. S41 in ESI[†]). The Hamiltonian for a linear trimer is described as follows, $H = -2J_1(S_1 \cdot S_2 + S_1 \cdot S_3) - 2J_2(S_2 \cdot S_3)$, J_1 and J_2 are the magnetic exchange integrals between two neighboring and two outer Mn(II)

centers, respectively. Since the shortest distance between the Mn_3 units is more than 12 Å, and π - π stacking interactions are present between the pyridyl rings of these chains (3.8 Å), thus, the interchain interactions (zJ) are included in the expression: $\chi_M^{\text{ic}} = \chi_M / (1 - zJ\chi_M / Ng^2\mu_B^2)$. The results from the best fit gives the values as follows: $g = 2.04$, $2J_1 = -3.4 \text{ cm}^{-1}$, $2J_2 = 0.25 \text{ cm}^{-1}$, $zJ = -0.02 \text{ cm}^{-1}$, and $R = 3.8 \times 10^{-6}$, where the agreement factor (R) is defined as $\Sigma(\chi_M^{\text{calcd}} - \chi_M^{\text{obs}})^2 / \Sigma(\chi_M^{\text{obs}})^2$.

The data of **3** were fitted according to the Curie-Weiss Law, giving the Curie constant $C = 17.34 \text{ cm}^3 \text{K mol}^{-1}$ and $\theta = -32.8 \text{ K}$ (Fig. S42, ESI[†]). In addition, using the same equation as was used for **2** resulted in the following data for **3**: $g = 2.12$, $2J_1 = -2.8 \text{ cm}^{-1}$, $2J_2 = 1.3 \text{ cm}^{-1}$, $zJ = -0.06 \text{ cm}^{-1}$, and $R = 9.1 \times 10^{-5}$. Despite the fact that **2** and **3** have different infinite structures, both consist of the Mn_3 cores furnished with the dtdn^{2-} ligands in the 2D network of **2** and the 1D double-stranded rod of **3**. The observed magnetic behavior is a combination of Mn^{II}-Mn couplings within the Mn_3 units and the weak inter-chain interactions.

The magnetic data of **5** were fitted to the Curie-Weiss Law and the Hamiltonian ($H = -2J_1 \sum S_i \cdot S_j$) for the 1D chain to give $C = 5.10 \text{ cm}^3 \text{K mol}^{-1}$, $\theta = -33.19 \text{ K}$ (Fig. S43 in ESI[†]), and $g = 2.07$, $2J_1 = -2.6 \text{ cm}^{-1}$, $\theta = 1.0 \text{ K}$, and $R = 5.1 \times 10^{-4}$. In contrast to **2** and **3**, no saturation is observed for **5** at 7 Tesla. The 1.8 K value of $1.01 \text{ N}\beta$ at 7 Tesla indicates residual magnetic moments within the Mn chain. The results suggest that the spins are arranged in an anti-parallel fashion, resulting in a singlet spin ground state (Fig. S44 in ESI[†]).

Conclusion

In this work, we report on the assembly of diverse disulfide ensembles in Mn-based CPs via the use of a series of disulfide derivatives. The suitable impetus from the ancillary N-donor coligands, possessing a subtle chelating effect and/or steric hindrance, can be utilized to tune the target structures having mononuclear, trinuclear clusters, and infinite metal oxide wires. Employing such a synthesis strategy under mild reaction conditions designed to retain the disulfide ensembles offers an effectively route to the construction of new metal-organic frameworks with self-triggered chirality and multiple metal clusters. These variable disulfide ensembles in CPs are currently astonishing and may provide an unusual insight into exploring their biomimetic behavior.

Acknowledgements

We are grateful to National Taipei University of Technology, Academia Sinica, Taiwan, and the Ministry of Science and Technology of Taiwan for financial support.

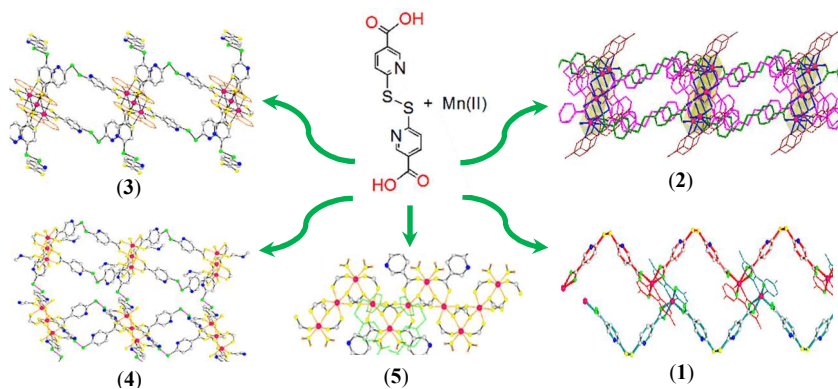
Notes and references

- (a) J. J. Pery IV, J. A. Perman and M. J. Zaworotko, *Chem. Soc. Rev.*, 2009, **38**, 1400; (b) M. O'Keeffe and O. M. Yaghi, *Chem. Rev.*, 2012, **112**, 675; (c) D. Zhao, D. J. Timmons, D. Yuan and H. C. Zhou, *Acc. Chem. Res.*, 2011, **44**, 123; (d) V. Guillerme, D. Kim, J. F. Eubank, R. Luebke, X. Liu,

- K. Adil, M. S. Lah and M. Eddaoudi, *Chem. Soc. Rev.*, 2014, **43**, 6141.
- 2 (a) J. Wang, S. L. Zheng, S. Hu, Y. H. Zhang and M. L. Tong, *Inorg. Chem.*, 2007, **46**, 795; (b) C. C. Stoumpos, R. Inglis, G. Karotsis, L. F. Jones, A. Collins, S. Parsons, C. J. Milios, G. S. Papaefstathiou and E. K. Brechin, *Cryst. Growth Des.*, 2009, **9**, 24; (c) Y. N. Zhang, P. Liu, Y. Y. Wang, L. Y. Wu, L. Y. Pang and Q. Z. Shi, *Cryst. Growth Des.*, 2011, **11**, 1531.
- 3 (a) L. Pan, H. Liu, X. Lei, X. Huang, D. H. Olson, N. J. Turro and J. Li, *Angew. Chem., Int. Ed.*, 2003, **42**, 542; (b) W. G. Lu, J. Z. Gu, L. Jiang, M. Y. Tan and T. B. Lu, *Cryst. Growth Des.*, 2008, **8**, 192; (c) H. A. Habib, J. Sanchiz and C. Janiak, *Dalton Trans.*, 2008, 4877; (d) R. Patra, H. M. Titi and I. Goldberg, *CrystEngComm*, 2013, **15**, 2863; (e) X. G. Guo, W. B. Yang, X. Y. Wu, Q. K. Zhang, L. Lin, R. M. Yu and C. Z. Lu, *CrystEngComm*, 2013, **15**, 3654.
- 4 (a) G. Férey, *Chem. Soc. Rev.*, 2008, **37**, 191; (b) S. Qiu and G. Zhu, *Coord. Chem. Rev.*, 2009, **253**, 2891; (c) D. J. Tranchemontagne, J. L. Mendoza-Cortes, M. O'Keefe and O. M. Yaghi, *Chem. Soc. Rev.*, 2009, **38**, 1257; (d) J. R. Li, Y. Ma, M. C. McCarthy, J. Sculley, J. Yu, H. K. Jeong, P. B. Balbuena and H. C. Zhou, *Coord. Chem. Rev.*, 2011, **255**, 1791; (e) H. C. Zhou, J. R. Long and O. M. Yaghi, *Chem. Rev.*, 2012, **112**, 673.
- 5 (a) P. M. Forster, N. Stock and A. K. Cheetham, *Angew. Chem., Int. Ed.*, 2005, **44**, 7608; (b) T. T. Luo, H. L. Tsai, S. L. Yang, Y. H. Liu, R. D. Yadav, C. C. Su, C. H. Ueng, L. G. Lin and K. L. Lu, *Angew. Chem., Int. Ed.*, 2005, **44**, 6063; (c) Q. Y. Liu, Y. L. Wang, Z. M. Shan, R. Cao, Y. L. Jiang, Z. J. Wang and E. L. Yang, *Inorg. Chem.*, 2010, **49**, 8191; (d) S. Henke, A. Schneemann, A. Wütscher and R. A. Fischer, *J. Am. Chem. Soc.*, 2012, **134**, 9464; (e) B. Zheng, J. H. Luo, F. Wang, Y. Peng, G. H. Li, Q. S. Huo and Y. L. Liu, *Cryst. Growth Des.*, 2013, **13**, 1033; (f) J. G. Ding, X. Zhu, Y. F. Cui, N. Liang, P. P. Sun, Q. Chen, B. L. Li and H. Y. Li, *CrystEngComm*, 2014, **16**, 1632.
- 6 (a) R. J. Kuppler, D. J. Timmons, Q. R. Fang, J. R. Li, T. A. Makal, M. D. Young, D. Yuan, D. Zhao, W. Zhuang and H. C. Zhou, *Coord. Chem. Rev.*, 2009, **253**, 3042; (b) T. T. Luo, H. C. Wu, Y. C. Jao, S. M. Huang, T. W. Tseng, Y. S. Wen, G. H. Lee, S. M. Peng and K. L. Lu, *Angew. Chem., Int. Ed.*, 2009, **48**, 9464; (c) J. M. Gotthardt, K. F. White, B. F. Abrahams, C. Ritchie and C. Boskovic, *Cryst. Growth Des.*, 2012, **12**, 4425; (d) C. D. Nicola, E. Forlin, F. Garau, M. Gazzano, A. Lanza, M. Monari, F. Nestola, L. Pandolfo, C. Pettinari, A. Zorzi and F. Zorzi, *Cryst. Growth Des.*, 2013, **13**, 126; (e) M. Li, D. Li, M. O'Keefe and O. M. Yaghi, *Chem. Rev.*, 2014, **114**, 1343.
- 7 (a) Z. Chen, D. L. Gao, C. H. Diao, Y. Liu, J. Ren, J. Chen, B. Zhao, W. Shi and P. Cheng, *Cryst. Growth Des.*, 2012, **12**, 1201; (b) Z. Zhang, J. F. Ma, Y. Y. Liu, W. Q. Kan and J. Yang, *Cryst. Growth Des.*, 2013, **13**, 4338; (c) S. Roy and K. Biradha, *Cryst. Growth Des.*, 2013, **13**, 3232; (d) W. G. Yuan, F. Xiong, H. L. Zhang, W. Tang, S. F. Zhang, Z. He, L. H. Jing and D. B. Qin, *CrystEngComm*, 2014, **16**, 7701.
- 8 (a) L. H. Cao, Y. L. Wei, Y. Yang, H. Xu, S. Q. Zang, H. W. Hou and T. C. W. Mak, *Cryst. Growth Des.*, 2014, **14**, 1827; (b) J. Q. Liu, J. Wu, Y. Y. Wang, J. T. Lin and H. Sakiyama, *CrystEngComm*, 2014, **16**, 3103; (c) X. Zhang, L. Fan, W. Zhang, W. Fan, L. Sun and X. Zhao, *CrystEngComm*, 2014, **16**, 3203; (d) Y. Yang, J. Yang, P. Du, Y. Y. Liu and J. F. Ma, *CrystEngComm*, 2014, **16**, 6380; (e) K. Molčanov, M. Jurić and B. Kojić-Prodić, *Dalton Trans.*, 2014, **43**, 7208.
- 9 (a) A. I. Derman, W. A. Prinz, D. Belin and J. Beckwith, *Science*, 1993, **262**, 1744; (b) M. Ruoppolo, F. Vinci, T. A. Klink, R. T. Raines and G. Marino, *Biochemistry*, 2000, **39**, 12033; (c) V. D. Nguyen, F. Hatahet, K. E. Salo, E. Enlund, C. Zhang and L. W. Ruddock, *Micro. Cell Fact.*, 2011, **10**, 1.
- 10 L. F. Ma, Y. Y. Wang, L. Y. Wang, D. H. Lu, S. R. Batten and J. G. Wang, *Cryst. Growth Des.*, 2009, **9**, 2036.
- 11 (a) J. Wang, Y. H. Zhang, H. X. Li, Z. J. Lin, and M. L. Tong, *Cryst. Growth Des.*, 2007, **7**, 2352; (b) F. Hofbauer and I. Frank, *Chem.–Eur. J.*, 2010, **16**, 5097; (c) Y. Bu, F. Jiang, S. Zhang, J. Ma, X. Li and M. Hong, *CrystEngComm*, 2011, **13**, 6323; (d) Q. Zhu, T. Sheng, C. Tan, S. Hu, R. Fu, and X. Wu, *Inorg. Chem.*, 2011, **50**, 7618; (e) A. B. Lago, R. Carballo, O. Fabelo, N. Fernández-Hermida, F. Lloret and E. M. Vázquez-López, *CrystEngComm*, 2013, **15**, 10550; (f) L. Wang, W. He and Z. Yu, *Chem. Soc. Rev.*, 2013, **42**, 599; (g) I. Lumb, M. S. Hundal and G. Hundal, *Inorg. Chem.*, 2014, **53**, 7770.
- 12 (a) H. F. Gilbert, *Advances in Enzymology*, 1990, **63**, 69; (b) H. F. Gilbert, *Methods Enzymol.*, 1995, **251**, 8; (c) H. B. Zhu and S. H. Gou, *Coord. Chem. Rev.*, 2011, **255**, 318; (d) H. B. Zhu, Y. F. Wu, Y. Zhao and J. Hu, *Dalton Trans.*, 2014, **43**, 17156.
- 13 (a) R. Horikoshi, T. Mochida and H. Moriyama, *Inorg. Chem.*, 2001, **40**, 2430; (b) R. Horikoshi and M. Mikuriya, *Cryst. Growth Des.*, 2005, **5**, 223; (c) N. de la Pinta, L. Fidalgo, G. Madariaga, L. Lezama and R. Cortés, *Cryst. Growth Des.*, 2012, **12**, 5069.
- 14 (a) F. M. Tabellion, S. R. Seidel, A. M. Arif and P. J. Stang, *J. Am. Chem. Soc.*, 2001, **123**, 7740; (b) A. J. Blake, N. R. Brooks, N. R. Champness, M. Crew, A. Deveson, D. Fenske, D. H. Gregory, L. R. Hanton, P. Hubberstey and M. Schröder, *Chem. Commun.*, 2001, 1432; (c) R. Horikoshi, T. Mochida, M. Kurihara and M. Mikuriya, *Cryst. Growth Des.*, 2005, **5**, 243; (d) L. F. Ma, L. Y. Wang and M. Du, *CrystEngComm*, 2009, **11**, 2593; (e) Y. N. Zhang, Y. Y. Wang, G. P. Yang, L. Hou and Q. Z. Shi, *Inorg. Chim. Acta*, 2010, **363**, 3413.
- 15 (a) T. W. Tseng, T. T. Luo, S. Y. Chen, C. C. Su, K. M. Chi and K. L. Lu, *Cryst. Growth Des.*, 2013, **13**, 510; (b) T. W. Tseng, T. T. Luo, C. C. Su, H. H. Hsu, C. I. Yang and K. L. Lu, *CrystEngComm*, 2014, **16**, 2626; (c) T. W. Tseng, T. T. Luo and K. H. Lu, *CrystEngComm*, 2014, **16**, 5516; (d) T. W. Tseng, M. L. Yang and T. T. Luo, *J. Solid. State Chem.*, 2015, **221**, 345.
- 16 Y. N. Zhang, Y. Y. Wang, L. Hou, P. Liu, J. Q. Liu and Q. Z. Shi, *CrystEngComm*, 2010, **12**, 3840.
- 17 (a) F. Li, L. Xu, B. Bi, X. Liu and L. Fan, *CrystEngComm*, 2008, **10**, 693; (b) C. E. Rowland, N. Belai, K. E. Knope and C. L. Cahill, *Cryst. Growth Des.*, 2010, **10**, 1390; (c) N. Yuan, T. L. Sheng, J. Zhang, C. B. Tian, S. M. Hu, X. H. Huang, F. Wang and X. T. Wu, *CrystEngComm*, 2011, **13**, 5951.
- 18 (a) G. M. Sheldrick, *SHELXS-97, Programs for X-ray Crystal Structure Solution*; University of Göttingen: Göttingen, Germany, 1997; (b) G. M. Sheldrick, *A Short History of SHELX*, *Acta Cryst.*, 2008, **A64**, 112.
- 19 A. L. Spek, *Acta Cryst.*, 2015, **C71**, 9.

Self-triggered conformations of disulfide ensembles in coordination polymers with multiple metal clusters

Tien-Wen Tseng, Tzuoo-Tsair Luo, Ying-Ru Shih, Jing-Wen Shen, Li-Wei Lee, Ming-Hsi Chiang, and Kuang-Lieh Lu



A series of coordination polymers were synthesized under mild conditions by the reaction of manganese(II) ions, the disulfide derivative, 6,6'-dithiodinic acid (H₂dtdn), and/or ancillary N-donor coligands, which provide a suitable impetus to direct the target coordination polymers to form mononuclear, trinuclear clusters and polymeric metal oxide wires, respectively. The disulfide ensembles in Mn-based MOFs with versatile connecting modes exhibit intrinsic biomimetic characteristics.

